

PM3 Analysis of Nitronc Cycloadditions to Methyl 4,4,4-Trifluoro-2-butenate

Kiyoshi Tanaka,* Tatsuya Imase, and Satoru Iwata

Faculty of Engineering, Seikei University, Musashino, Tokyo 180

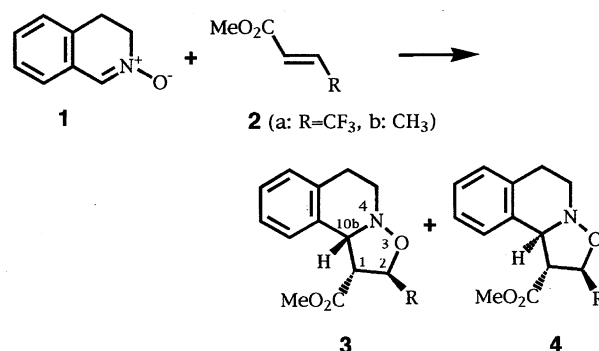
(Received January 12, 1996)

3,4-Dihydroisoquinoline *N*-oxide (**1**) cycloadded with methyl 4,4,4-trifluoro-2-butenate at 20 °C to give a mixture of the cycloadduct with a 1,10b-*cis*-configuration, methyl (1*R*^{*}, 2*R*^{*}, 10b*R*^{*})-2-trifluoromethyl-1,5,6,10b-tetrahydro-2*H*-isoxazolo[3,2-*a*]isoquinoline-1-carboxylate, and its stereoisomer with a 1,10b-*trans*-configuration in a ratio of 3 : 1. Nitronc **1** cycloadded with methyl 2-butenate to afford the cycloadduct with a 1,10b-*cis*-configuration exclusively. The stereoselectivity in the cycloadditions was reproduced by calculations of the transition structures by the PM3 method.

Stereoselectivity in nitronc cycloadditions with 4,4,4-trifluoro-2-butenates seems to depend on the substituents of the used 4,4,4-trifluoro-2-butenates and nitroncs. For example, *C*-phenyl-*N*-methylnitronc was reported to react with methyl 4,4,4-trifluoro-2-butenate (**2a**) to give predominantly isoxazolidine with a 4-ester-3,4-*cis*-configuration¹⁾ and with 3-silyloxy- or -hydroxy substituted 4,4,4-trifluoro-2-butenate to produce exclusively isoxazolidine with a 4-ester-3,4-*trans*-configuration.²⁾ On the other hand, it was reported that cycloaddition of *C*, *N*-diphenylnitronc with ethyl 4,4,4-trifluoro-2-butenate produced 4-ester-3,4-*trans*-isoxazolidine and, on the contrary, *C*-ethoxycarbonyl-*N*-benzyl-nitronc afforded 4-ester-3,4-*cis*-isoxazolidine.³⁾ Discussion of the nitronc stereoselectivity was, however, restricted because of the possible *E*-*Z* isomerization of the nitronc upon cycloaddition.^{4,5)} The possibility of nitronc *E*-*Z* isomerization prompted us to explore using the configurationally-fixed nitronc, 3,4-dihydroisoquinoline *N*-oxide (**1**). In this paper, we wish to demonstrate stereoselectivity in the cycloadditions of nitronc **1** with trifluorobutenate **2a** and to interpret the stereoselectivity on the basis of a PM3 analysis.

Results and Discussion

The reaction of nitronc **1** with trifluorobutenate **2a** in toluene at 20 °C for 20 h afforded a mixture of the cycloadduct with a 1,10b-*cis*-configuration, methyl (1*R*^{*}, 2*R*^{*}, 10b*R*^{*})-2-trifluoromethyl-1,5,6,10b-tetrahydro-2*H*-isoxazolo[3,2-*a*]isoquinoline-1-carboxylate (**3a**), and its stereoisomer **4a** with a 1,10b-*trans*-configuration in a ratio of 3 : 1 (Table 1), their regioisomers being not detected in the reaction mixture (Scheme 1). The structure of **4a** was unequivocally determined by X-ray analysis (Fig. 1), along with the conventional spectroscopic data and elemental analysis. It should be noted that X-ray analysis indicates the conformation of the tetrahydropyridine ring in **4a** to be chair-type, rather than boat-type (Tables 2, 3, and 4). The configuration of major product **3a** was determined by the chemical shifts of the methyl protons



Scheme 1.

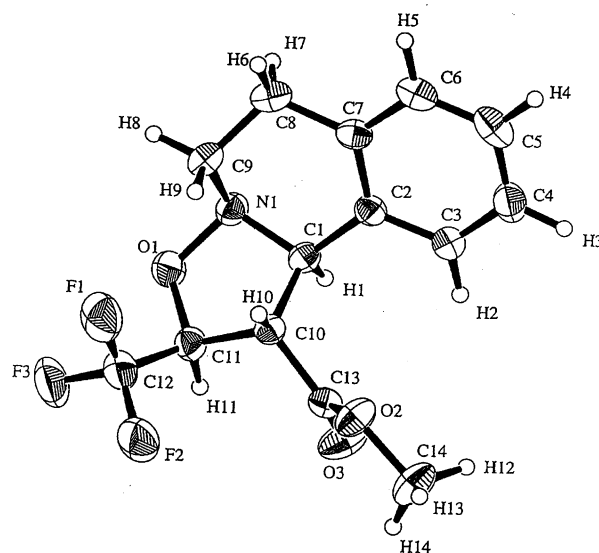


Fig. 1. ORTEP drawing of **4a**.

in 1-methoxycarbonyl group; that is, the shielded chemical shift ($\delta = 3.28$) of **3a**, compared with that ($\delta = 3.86$) of **4a**, is ascribed to a 1,10b-*cis*-configuration. The similar reaction under a more elevated temperature produced **4a** exclusively.

Table 1. Yields and Product Ratios in Cycloadditions of Nitronc 1 with 2-Butenoates 2

| 2-Butenoate | Reaction temp/°C | Total yield/% | Ratio (3 / 4) |
|-------------|------------------|---------------|---------------|
| 2a | 20 | 71 | 75/25 |
| | 80 | 70 | 0/100 |
| 2b | 20 | 57 | 100/0 |
| | 80 | 63 | 71/29 |

Table 2. Atomic Coordinates and $B_{\text{iso}}/B_{\text{eq}}$ for **4a**

| Atom ^{a)} | x | y | z | B_{eq} ^{b)} |
|--------------------|------------|------------|------------|-------------------------------|
| F(1) | 0.5512(2) | 0.13031(8) | 0.2156(1) | 7.89(5) |
| F(2) | 0.3987 | 0.0352(2) | 0.19031(8) | 8.51(5) |
| F(3) | 0.5700 | 0.0500 | 0.3808(2) | 8.21(5) |
| O(1) | 0.3947 | 0.1727 | 0.4578 | 4.79(4) |
| O(2) | 0.0033(1) | 0.1184 | 0.0611 | 5.21(4) |
| O(3) | -0.0353(1) | 0.0800(1) | 0.2783 | 6.27(5) |
| N(1) | 0.3146(1) | 0.2431(2) | 0.4285(1) | 4.12(5) |
| C(1) | 0.1522(3) | 0.2244(1) | 0.3458(2) | 3.60(5) |
| C(2) | 0.06899(8) | 0.2879(3) | 0.2659(1) | 3.64(5) |
| C(3) | -0.0987(4) | 0.28245(8) | 0.2084(3) | 4.57(6) |
| C(4) | -0.1779(2) | 0.3389(5) | 0.12963(9) | 5.49(7) |
| C(5) | -0.0882(1) | 0.4014(2) | 0.1116(5) | 5.72(7) |
| C(6) | 0.0771(3) | 0.4075(1) | 0.1704(2) | 5.02(7) |
| C(7) | 0.1583 | 0.3512(3) | 0.2478(1) | 4.00(6) |
| C(8) | 0.3383 | 0.3589 | 0.3145(2) | 4.96(6) |
| C(9) | 0.4218 | 0.2855 | 0.3407 | 4.55(6) |
| C(10) | 0.1945(2) | 0.1599 | 0.2502 | 3.41(5) |
| C(11) | 0.3223(3) | 0.1204(1) | 0.3548 | 4.16(6) |
| C(12) | 0.4610(1) | 0.0845(3) | 0.2858(1) | 5.76(7) |
| C(13) | 0.0429(3) | 0.1141(2) | 0.2009(3) | 3.78(5) |
| C(14) | -0.1481(1) | 0.0794(4) | 0.0020(2) | 6.35(7) |
| H(1) | 0.0817(4) | 0.20736(8) | 0.4112(3) | 2.4379(2) |
| H(2) | -0.1605(2) | 0.2396(5) | 0.2230(1) | 3.7839(4) |
| H(3) | -0.2978(7) | 0.333(1) | 0.1(3) | 6.3 |
| H(4) | -0.140(2) | 0.4402(8) | 0.053(1) | 6.4(4) |
| H(5) | 0.1412 | 0.452(2) | 0.158(1) | 5.724(2) |
| H(6) | 0.4020 | 0.3877 | 0.247(2) | 6.034(1) |
| H(7) | 0.3401 | 0.3834 | 0.4049 | 4.918(2) |
| H(8) | 0.5304 | 0.2905 | 0.4032 | 5.1 |
| H(9) | 0.4422 | 0.2619 | 0.2442 | 5.3 |
| H(10) | 0.2459 | 0.1759 | 0.1687 | 3.1 |
| H(11) | 0.2629 | 0.0823 | 0.4046 | 4.7 |
| H(12) | -0.2500 | 0.1043 | 0.0414 | 12.9 |
| H(13) | -0.1(4) | 0.0759 | -0.0887 | 8.3 |
| H(14) | -0.145(2) | 0.0(4) | 0.0499 | 12.5 |

a) Number of the atom refers to that in ORTEP drawing (Fig. 1).

b) $B_{\text{eq}} = (8/3)\pi^2 \{U_{11}(aa^*)^2 + U_{22}(bb^*)^2 + U_{33}(cc^*)^2 + 2U_{12}aa^*bb^*\cos\gamma + 2U_{13}aa^*cc^*\cos\beta + 2U_{23}bb^*cc^*\cos\alpha\}$.

Although the isolated **3a** is stable at room temperature, it converted into **4a** at an elevated temperature. ¹H NMR analysis using 1,1,2,2-tetrachloroethane as an internal standard indicated that heating the isolated **3a** in deuteriochloroform at 60 °C for 9 h produced a mixture of **3a**, **4a**, and **2a** in a 45 : 35 : 20 ratio. The product ratio changed to 25 : 55 : 18 on prolonged heating for 10 more hours. These facts show that the kinetically controlled product **3a** epimerized to the thermodynamically controlled product **4a** via 1,3-dipolar cycloreversion, as reported in our previous paper concerning C-phenyl-N-methylnitronc cycloadditions,¹⁾ and that the 3 : 1 product ratio of **3a** to **4a** at 20 °C is the primary product ratio

in the cycloaddition.

Cycloaddition with methyl 2-butenate proceeded stereospecifically to give one cycloadduct, methyl (1*R**, 2*S**, 10*bR**)-2-methyl-1,5,6,10*b*-tetrahydro-2*H*-isoxazolo[3,2-*a*]-isoquinoline-1-carboxylate (**3b**), exclusively.⁶⁾ The stereospecificity of the cycloaddition was relaxed at 80 °C, affording stereoisomer **4b** in a 29% ratio as a by-product. Epimerization similar to that described above was observed in this case; that is, the isolated **3b** was heated at 80 °C for 24 h in deuteriochloroform to give a mixture of **3b**, **4b**, and **2b** in a 42 : 29 : 29 ratio. From the fact of epimerization of **3b** into **4b** at an elevated temperature and the spectroscopic feature

Table 3. Bond Lengths for **4a**

| Atom ^{a)} | Atom ^{a)} | Distance/Å | Atom ^{a)} | Atom ^{a)} | Distance/Å |
|--------------------|--------------------|------------|--------------------|--------------------|------------|
| F(1) | C(12) | 1.330(4) | C(2) | C(3) | 1.385(3) |
| F(2) | C(12) | 1.331(4) | C(2) | C(7) | 1.387(6) |
| F(3) | C(12) | 1.332(4) | C(3) | C(4) | 1.385(7) |
| O(1) | N(1) | 1.460(4) | C(4) | C(5) | 1.376(8) |
| O(1) | C(11) | 1.437(2) | C(5) | C(6) | 1.371(3) |
| O(2) | C(13) | 1.314(3) | C(6) | C(7) | 1.384(5) |
| O(2) | C(14) | 1.458(4) | C(7) | C(8) | 1.502(1) |
| O(3) | C(13) | 1.187(3) | C(8) | C(9) | 1.5150(4) |
| N(1) | C(1) | 1.470(3) | C(10) | C(11) | 1.516(2) |
| N(1) | C(9) | 1.474(3) | C(10) | C(13) | 1.502(3) |
| C(1) | C(2) | 1.502(5) | C(11) | C(12) | 1.495(3) |
| C(1) | C(10) | 1.549(2) | | | |
| C(1) | H(1) | 0.931 | C(9) | H(8) | 0.991 |
| C(3) | H(2) | 0.948 | C(9) | H(9) | 1.033 |
| C(4) | H(3) | 1.000 | C(10) | H(10) | 0.953 |
| C(5) | H(4) | 0.965 | C(11) | H(11) | 0.992 |
| C(6) | H(5) | 0.977 | C(14) | H(12) | 1.035 |
| C(8) | H(6) | 1.004 | C(14) | H(13) | 0.854 |
| C(8) | H(7) | 0.959 | C(14) | H(14) | 0.949 |

a) Number of the atom refers to that in ORTEP drawing (Fig. 1).

of the chemical shifts of the methyl protons in 1-methoxycarbonyl groups of **3b** and **4b**, the configurations of **3b** and **4b** were determined to be 1,10b-*cis* and -*trans*, respectively.

Considerable formation of stereoisomeric 1,10b-*trans*-cycloadduct **4a** in the addition with trifluoro-2-butenate under kinetically controlled conditions is in sharp contrast to the exclusive formation of 1,10b-*cis*-cycloadduct **3b** with 2-butenate.

The difference in stereoselectivity is well reproduced by calculations of the transition states. It is reported that *ab initio* calculations concerning 1,3-dipolar compounds seem to be in better agreement with experimental data than semiempirical calculations such as AM1 and PM3 methods.⁷⁾ However *ab initio* calculations are still limited to small molecules because of the limitations of computer capacity. And nitron reactivity such as pyridine *N*-oxide regioselectivity is reported to be well explained by PM3 calculations.⁸⁾ Therefore an explanation of the stereoselectivity in the cycloadditions of nitron **1** was attempted on the basis of PM3 calculations.⁹⁾

Here we assume a concerted mechanism for the nitron cycloadditions, which means excluding the occurrence of biradical intermediates.^{10–13)} The potential energy surface for the interaction of **1** with trifluoro-2-butenate or with 2-butenate was searched by RHF calculations having a close-shell nature on the reaction path. By an optimized double search between 1.7–3.0 Å for two newly formed bonds, one stationary point was found, refined by NLLSQ calculations, and characterized by one negative vibrational frequency which supports it as a true transition state. Calculated properties of transition structure **3[‡]** (ester-*endo*) and **4[‡]** (ester-*exo*) are summarized in Table 5 and Fig. 2, together with those of the ground states of the reactants and products.

Calculated results of the transition structures are all for **3[‡]** and **4[‡]** with the chair-type conformation of the tetrahydropyridine ring, since the calculated heats of formation of the

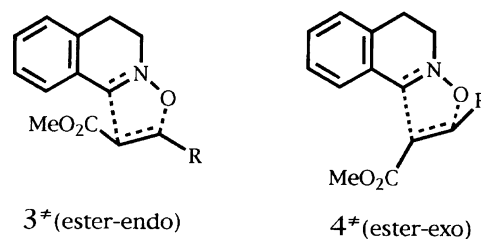


Fig. 2. Transition structure.

corresponding **3[‡]** and **4[‡]** with the boat-type conformation of the tetrahydropyridine ring are smaller than those of chair-type **3[‡]** and **4[‡]**.

The activation enthalpies ($\Delta\Delta H_f$ values in Table 5) into cycloadducts **3a**, **4a**, **3b**, and **4b**, along with their heats of formation, support that 1,10b-*cis*-cycloadducts **3a** and **3b** are kinetically controlled products and 1,10b-*trans*-cycloadducts **4a** and **4b** are thermodynamically controlled products, which is well consistent with experimental results. It should be noted that the regioisomeric *endo*- and *exo*-transition structures were calculated and their activation enthalpies were found to be rather bigger than those of the corresponding **3[‡]** and **4[‡]**. Appreciable formation of **4a** from trifluoro-2-butenate under kinetically controlled reaction conditions, contrasting to the exclusive formation of **3b** from 2-butenate, is, however, not explained only by the activation enthalpy. Consideration of the activation entropy (the ΔS value in Table 5), which leads to the activation Gibbs energy (the ΔG value in Table 5), might be necessary. The smaller difference in the activation Gibbs energy between **3a[‡]** and **4a[‡]**, compared with that between **3b[‡]** and **4b[‡]**, reproduces the substantial formation of **4a**.

From calculations of the transition structures, the newly created C–O bond is formed to a greater extent than another C–C bond, even though the corresponding C–O bond length

Table 4. Bond Angles for **4a**

| Atom ^{a)} | Atom ^{a)} | Atom ^{a)} | Angle/° | Atom ^{a)} | Atom ^{a)} | Atom ^{a)} | Angle/° |
|--------------------|--------------------|--------------------|----------|--------------------|--------------------|--------------------|-----------|
| N(1) | O(1) | C(11) | 109.8(1) | C(7) | C(8) | C(9) | 111.3(2) |
| C(13) | O(2) | C(14) | 116.3(2) | N(1) | C(9) | C(8) | 107.0(1) |
| O(1) | N(1) | C(1) | 103.2(3) | C(1) | C(10) | C(11) | 99.7(1) |
| O(1) | N(1) | C(9) | 108.0(1) | C(1) | C(10) | C(13) | 113.0(2) |
| C(1) | N(1) | C(9) | 111.1(1) | C(11) | C(10) | C(13) | 112.7(1) |
| N(1) | C(1) | C(2) | 113.0(3) | O(1) | C(11) | C(10) | 107.5(2) |
| N(1) | C(1) | C(10) | 104.5(2) | O(1) | C(11) | C(12) | 109.2(2) |
| C(2) | C(1) | C(10) | 115.0(2) | C(10) | C(11) | C(12) | 114.00(8) |
| C(1) | C(2) | C(3) | 119.2(3) | F(1) | C(12) | F(2) | 106.4(1) |
| C(1) | C(2) | C(7) | 121.0(1) | F(1) | C(12) | F(3) | 106.7(1) |
| C(3) | C(2) | C(7) | 119.8(3) | F(1) | C(12) | C(11) | 113.4(4) |
| C(2) | C(3) | C(4) | 120.8(3) | F(2) | C(12) | F(3) | 106.7(4) |
| C(3) | C(4) | C(5) | 119.0(2) | F(2) | C(12) | C(11) | 110.9(1) |
| C(4) | C(5) | C(6) | 120.4(3) | F(3) | C(12) | C(11) | 112.3(1) |
| C(5) | C(6) | C(7) | 121.2(3) | O(2) | C(13) | O(3) | 123.9(2) |
| C(2) | C(7) | C(6) | 118.7(1) | O(2) | C(13) | C(10) | 111.5(2) |
| C(2) | C(7) | C(8) | 120.3(3) | O(3) | C(13) | C(10) | 124.6(2) |
| C(6) | C(7) | C(8) | 120.9(3) | | | | |
| N(1) | C(1) | H(1) | 106.94 | N(1) | C(9) | H(9) | 114.98 |
| C(2) | C(1) | H(1) | 109.10 | C(8) | C(9) | H(8) | 110.42 |
| C(10) | C(1) | H(1) | 107.87 | C(8) | C(9) | H(9) | 110.16 |
| C(2) | C(3) | H(2) | 119.73 | H(8) | C(9) | H(9) | 110.13 |
| C(4) | C(3) | H(2) | 119.46 | C(1) | C(10) | H(10) | 111.42 |
| C(3) | C(4) | H(3) | 119.03 | C(11) | C(10) | H(10) | 110.48 |
| C(5) | C(4) | H(3) | 121.96 | C(13) | C(10) | H(10) | 109.28 |
| C(4) | C(5) | H(4) | 119.75 | O(1) | C(11) | H(11) | 109.63 |
| C(6) | C(5) | H(4) | 119.78 | C(10) | C(11) | H(11) | 108.92 |
| C(5) | C(6) | H(5) | 120.65 | C(12) | C(11) | H(11) | 107.59 |
| C(7) | C(6) | H(5) | 118.14 | O(2) | C(14) | H(12) | 106.89 |
| C(7) | C(8) | H(6) | 108.28 | O(2) | C(14) | H(13) | 108.05 |
| C(7) | C(8) | H(7) | 109.32 | O(2) | C(14) | H(14) | 106.26 |
| C(9) | C(8) | H(6) | 109.37 | H(12) | C(14) | H(13) | 119.27 |
| C(9) | C(8) | H(7) | 108.41 | H(12) | C(14) | H(14) | 101.86 |
| H(6) | C(8) | H(7) | 110.15 | H(13) | C(14) | H(14) | 113.63 |
| N(1) | C(9) | H(8) | 103.89 | | | | |

a) Number of the atom refers to that in ORTEP drawing (Fig. 1).

Table 5. PM3 Calculated Properties of Transition Structures and Products

| | 3a [‡] | 4a [‡] | 3b [‡] | 4b [‡] | 3a | 4a | 3b | 4b |
|---|-----------------|-----------------|-----------------|-----------------|----------|---------------------|---------|---------|
| ΔH_f (kcal mol ⁻¹) ^{a)} | -164.855 | -163.638 | -13.403 | -12.651 | -215.311 | -217.043 | -58.712 | -62.925 |
| S (cal K ⁻¹ mol ⁻¹) ^{a)} | 143.428 | 145.479 | 131.525 | 130.187 | — | — | — | — |
| $\Delta\Delta H_f$ (kcal mol ⁻¹) ^{b)} | 28.650 | 29.867 | 32.810 | 33.562 | — | — | — | — |
| ΔS (cal K ⁻¹ mol ⁻¹) ^{c)} | -52.040 | -49.990 | -47.750 | -49.088 | — | — | — | — |
| ΔG (kcal mol ⁻¹) ^{d)} | 43.898 | 44.514 | 46.801 | 47.945 | — | — | — | — |
| Formed bond lengths (Å) | | | | | | | | |
| C2–O3 ^{e)} | 1.769 | 1.708 | 1.810 | 1.852 | 1.401 | 1.404 ^{f)} | 1.432 | 1.425 |
| C1–C10b ^{e)} | 2.351 | 2.469 | 2.302 | 2.308 | 1.549 | 1.549 ^{f)} | 1.539 | 1.538 |
| Formed bond order | | | | | | | | |
| C2–O3 ^{e)} | 0.483 | 0.532 | 0.457 | 0.416 | 1.022 | 1.016 | 0.983 | 0.989 |
| C1–C10b ^{e)} | 0.232 | 0.184 | 0.255 | 0.252 | 0.946 | 0.949 | 0.962 | 0.966 |
| Negative frequency (cm ⁻¹) | 595.28 i | 521.05 i | 666.57 i | 677.02 i | — | — | — | — |

a) Values at 293 K. b) $\Delta\Delta H_f = \Delta H_f$ (transition structure) – ΔH_f (reactant); ΔH_f (reactant)/kcal mol⁻¹/at 293 K = 31.449 (**1**), –224.954 (**2a**), and –77.662 (**2b**). c) $\Delta S = S$ (transition structure) – S (reactant); S (reactant)/cal K⁻¹ mol⁻¹/at 293 K = 89.030 (**1**), 106.439 (**2a**), and 90.246 (**2b**). d) $\Delta G = \Delta\Delta H_f - T\Delta S$ (at 293 K). e) Number of the atom refers to that in Scheme 1. f) Bond lengths by X-ray analysis are 1.437 Å (C2–O3) and 1.549 Å (C1–C10b).

of the final product **4a** is estimated to be slightly shorter than that shown by X-ray analysis. For example, the C–O

and C–C distance of ester-*endo*-transition structure **3b[‡]** are 1.810 and 2.302 Å, respectively, and inspection of the bond

orders of **3b**[‡] and cycloadduct **3b** reveals that the C–O bond is 46.5% formed at the transition state and fairly more advanced than the C–C bond (26.5%) (Table 5). A similar unsymmetrical approach is depicted for **3a**[‡]; that is, 1.769 Å (47.2% bond formed) is estimated for the C–O distance and 2.351 Å (24.5%) for the C–C distance. On the other hand, a longer C–O distance (1.852 Å) is estimated for ester-*exo*-transition structure **4b**[‡], which is in sharp contrast to the shorter estimated C–O distance (1.708 Å) for **4a**[‡].

The exclusive formation of **3b** under kinetically controlled reaction conditions is easily interpreted by the stabilizing secondary orbital interactions of the ester carbonyl group with the HOMO lobe on the nitrogen atom and with the phenyl ring in ester-*endo*-transition structure **3b**[‡].^{14,15} In ester-*exo*-transition structure **4b**[‡], steric repulsion between the 2-methyl group and the tetrahydropyridine ring seems to lengthen the C–O distance and to increase the instability. On the contrary, the shortened C–O distance in ester-*exo*-transition structure **4a**[‡] might be attained by a balance of the steric repulsion caused by the more bulky trifluoromethyl group and the stabilizing interactions such as an orbital interaction between the trifluoromethyl group and the HOMO lobe of the nitrogen atom.^{16,17} Shortening the C–O distance seems to increase the activation enthalpy and to decrease the activation Gibbs energy, compared with **4b**[‡], leading to the substantial formation of **4a**.

In conclusion, calculations of the transition structures and products by the PM3 method reproduced the experimental results that 1,10b-*cis*-cycloadducts **3a** and **3b** are kinetically controlled products and 1,10b-*trans*-cycloadducts **4a** and **4b** are thermodynamically controlled products. Appreciable formation of **4a** from trifluoro-2-butenate under kinetically controlled reaction conditions is ascribed to the shortened C–O distance in **4a**[‡], compared with that of **3a**[‡], which brings about not only an increase of the activation enthalpy, but also a decrease of the activation Gibbs energy.

Experimental

The IR spectra were recorded on a JASCO A-100 spectrometer and samples were run as potassium bromide pellets. The ¹H NMR spectra were measured with a JEOL JNM-GX270 spectrometer (270 MHz) using tetramethylsilane as an internal standard, the chemical shifts being given in δ/ppm downfield. Samples were prepared by dissolving in deuteriochloroform. 2-Butenoates **2a** and **2b** are commercially available. Nitron **1** was prepared by the previously reported method,¹⁸ its ¹H NMR data being consistent with the reported data.

X-ray Crystal Structural Analysis of 4a. A colorless plate crystal of **4a** (C₁₄H₁₄NF₃O₃) having approximate dimensions of 0.68×0.30×0.15 mm was mounted on a glass fiber. All measurements were made on a Rigaku AFC5S diffractometer with graphite monochromated Cu Kα radiation.

Cell constants and an orientation matrix for data collection, obtained from a least-squares refinement using the setting angles of 25 carefully centered reflections in the range 64.46 < 2θ < 69.81° corresponded to a primitive monoclinic cell with dimensions: *a* = 7.951(3), *b* = 18.445(5), *c* = 9.365(3) Å, β = 96.48(3)°, and *V* = 1364.7(6) Å³. For *Z* = 4 and F.W. = 301.26, the calculated

density is 1.47 g cm^{−3}. The systematic absence of: *h*0*l*: *l* ≠ 2*n*, 0*k*0: *k* ≠ 2*n* uniquely determine the space group to be *P*21/*c* (#14).

The data were collected at a temperature of 23 ± 1 °C using the ω–2θ scan technique to a maximum 2θ value of 120.1°. Omega scans of several intense reflections, made prior to data collection, had an average width at half-height of 0.23° with a take-off angle of 6.0°. Scans of (1.52 + 0.30 tan θ)° were made at a speed of 8.0° min^{−1} (in omega). The weak reflections (*I* < 5.0σ(*I*)) were rescanned (maximum of 2 scans) and the counts were accumulated to ensure good counting statistics. Stationary background counts were recorded on each side of the reflection. The ratio of peak counting time to background counting time was 2 : 1. The diameter of the incident beam collimator was 1.0 mm, the crystal-to-detector distance was 285 mm, and the detector aperture was 6.0×6.0 mm (horizontal×vertical).

Of the 2277 reflections which were collected, 2111 were unique (*R*_{int} = 0.030). The intensities of three representative reflections were measured after every 150 reflections. No decay correction was applied.

The linear absorption coefficient, μ, for Cu Kα radiation is 11.3 cm^{−1}. An empirical absorption correction based on azimuthal scans of several reflections was applied which resulted in transmission factors ranging from 0.79 to 1.00. The data were corrected for Lorentz and polarization effects. A correction for secondary extinction was applied (coefficient = 6.42873e − 06).

The structure was solved by direct methods¹⁹ and expanded using Fourier techniques.²⁰ The non-hydrogen atoms were refined anisotropically. Some hydrogen atoms were refined isotropically, the rest were included in fixed positions. The final cycle of full-matrix least-squares refinement (function minimized: Σw(|*F*_o| − |*F*_c|)²) was based on 1545 observed reflections (*I* > 3.00σ(*I*)) and 290 variable parameters and converged with unweighted and weighted agreement factors of *R* = 0.035 and *R*_w = 0.023, respectively. All calculations were performed using the teXsan program²¹ which used the atomic scattering factors taken from "International Tables for X-ray Crystallography".²² The atom coordinates are listed in Table 2 and bond lengths and angles are given in Tables 3 and 4, respectively.

Cycloaddition of 1 with Methyl Trifluoro-2-butenate 2a. A solution of **1** (0.67 g, 4.53 mmol) and **2a** (0.58 g, 3.78 mmol) in 20 cm³ of toluene was stirred at 20 °C for 20 h and the solvent was then removed. The resulting oil was chromatographed on silica gel (hexane–ethyl acetate, 10/1) to give 0.18 g (53% yield) of **3a** and 0.03 g (18% yield) of **4a**. Each solid was purified by recrystallization from hexane–ethyl acetate.

3a: Mp 72–73 °C, ¹H NMR δ = 7.20 (4H, m), 5.13 (1H, dq, *J* = 6.1 and 6.1 Hz), 4.98 (1H, d, *J* = 9.8 Hz), 3.88 (1H, dd, *J* = 9.8 and 6.1 Hz), 3.58 (1H, ddd, *J* = 10.8, 10.8, and 4.3 Hz), 3.31 (1H, m), 3.28 (3H, s), 3.03 (1H, ddd, *J* = 16.6, 10.8, and 5.4 Hz), and 2.84 (1H, dt, *J* = 16.6 and 4.3 Hz); IR 1740 (C=O) and 1200–1140 cm^{−1} (CF₃). Found: C, 55.87; H, 4.72; N, 4.16%. Calcd for C₁₄H₁₄NF₃O₃: C, 55.82; H, 4.68; N, 4.65%.

4a: Mp 121–122 °C, ¹H NMR δ = 7.22 (3H, m), 6.96 (1H, m), 4.93 (1H, dm, *J* = 8.6 Hz), 4.78 (1H, dq, *J* = 8.6 and 6.5 Hz), 3.86 (3H, s), 3.61 (1H, dd, *J* = 8.6 and 8.6 Hz), 3.35 (1H, m), 3.26 (1H, m), and 2.97 (2H, t, *J* = 5.4 Hz); IR 1740 (C=O) and 1200–1140 cm^{−1} (CF₃). Found: C, 56.10; H, 4.58; N, 4.59%. Calcd for C₁₄H₁₄NF₃O₃: C, 55.82; H, 4.68; N, 4.65%.

A solution of **1** (0.90 g, 6.10 mmol) and **2a** (0.87 g, 5.66 mmol) in 30 cm³ of toluene was heated with stirring at 80 °C for 22 h. The usual work-up gave 1.2 g (70% yield) of **4a**.

Cycloaddition of 1 with Methyl 2-Butenoate 2b. A solution

of **1** (0.67 g, 4.53 mmol) and **2a** (0.38 g, 3.78 mmol) in 20 cm³ of toluene was stirred at 20°C for 43 h. The solvent was evaporated under reduced pressure to leave a residue. The resulting residue was chromatographed on silica gel (hexane–ethyl acetate, 4/1) to give 0.53 g (57% yield) of **3b**.

A similar reaction was performed at 80 °C for 24 h using a solution of **1** (0.67 g, 4.53 mmol) and **2a** (0.38 g, 3.78 mmol) in 20 cm³ of toluene. The solvent was removed and the resulting oil was chromatographed on silica gel (hexane–ethyl acetate, 3/1), affording 0.59 g (63% total yield) of a mixture of **3b** and **4b** in a ratio of 71/29 (by ¹H NMR analysis). Product **4b** was isolated by careful column chromatography. **3b** and **4b** were each purified by recrystallization from hexane–ethyl acetate.

3b: Mp 119–120 °C; ¹H NMR δ = 7.20 (4H, m), 4.97 (1H, d, J = 10.3 Hz), 4.86 (1H, dq, J = 7.6 and 7.6 Hz), 3.68 (1H, ddd, J = 11.7, 9.8, and 3.9 Hz), 3.37 (1H, dd, J = 10.3 and 7.6 Hz), 3.29 (3H, s), 3.24 (1H, m), 3.07 (1H, ddd, J = 16.4, 11.7, and 5.1 Hz), 2.84 (1H, b.d, J = 16.4 Hz), and 1.45 (3H, d, J = 7.6 Hz); IR 1720 cm⁻¹ (C=O). Found: C, 67.83; H, 7.22; N, 5.21%. Calcd for C₁₄H₁₇NO₃: C, 68.00; H, 6.93; N, 5.66%.

4b: Mp 46–47 °C; ¹H NMR δ = 7.15 (4H, m), 5.00 (1H, d, J = 6.6 Hz), 4.35 (1H, dq, J = 8.3 and 6.1 Hz), 3.80 (3H, s), 3.47 (1H, ddd, J = 12.8, 4.5, and 4.5 Hz), 3.20 (1H, ddd, J = 12.8, 8.8, and 4.2 Hz), 3.05 (1H, m), 3.00 (1H, dd, J = 8.3 and 6.6 Hz), 2.65 (1H, ddd, J = 15.9, 4.5, and 4.2 Hz), and 1.35 (3H, d, J = 6.1 Hz); IR 1720 cm⁻¹ (C=O). Found: C, 67.84; H, 6.96; N, 5.55%. Calcd for C₁₄H₁₇NO₃: C, 68.00; H, 6.93; N, 5.66%.

We express heartfelt thanks to Professor T. Tsubomura and Dr. K. Sakai for the X-ray analysis.

References

- 1) K. Tanaka, T. Mori, and K. Mitsunashi, *Bull. Chem. Soc. Jpn.*, **66**, 263 (1993); K. Tanaka, T. Mori, and K. Mitsunashi, *Chem. Lett.*, **1989**, 1115.
- 2) J. P. Bégué, D. Bonnet-Delpon, and T. Lequeux, *J. Chem. Soc., Perkin Trans. 1*, **1991**, 2888.
- 3) P. Bravo, L. Bruché, A. Mele, and G. Zecchi, *J. Chem. Res.*, **1991**, (S) 81, (M) 719; P. Bravo, L. Bruché, G. Fronza, and G. Zecchi, *Tetrahedron*, **48**, 9775 (1992).
- 4) L. W. Boyle, M. J. Peagram, and G. H. Whitham, *J. Chem. Soc. B*, **1971**, 1728.
- 5) A. Padwa, L. Fisera, K. F. Koehler, A. Rodriguez, and G. S. K. Wong, *J. Org. Chem.*, **49**, 276 (1984).
- 6) A kinetic aspect of this cycloaddition was reported, see: R. Huisgen, H. Seidl, and I. Bruning, *Chem. Ber.*, **102**, 1102 (1969).
- 7) R. Sustmann, W. Sicking, and R. Huisgen, *J. Org. Chem.*, **58**, 82 (1993).
- 8) T. Matsuoka, K. Harano, and T. Hisano, *Heterocycles*, **37**, 257 (1994).
- 9) The calculations were carried out by "CACHÉ MOPAC Ver. 3.5.1," J. P. Stewart, *QCPE Bull.*, **9**, 10 (1989).
- 10) R. Huisgen, *J. Org. Chem.*, **41**, 403 (1976).
- 11) K. N. Houk, J. Sims, R. E. Duke, Jr., R. W. Strozier, and J. K. George, *J. Am. Chem. Soc.*, **95**, 7287 (1973); K. N. Houk, *Acc. Chem. Res.*, **8**, 361 (1975).
- 12) R. Sustmann, *Tetrahedron Lett.*, **1971**, 2717.
- 13) J. J. W. McDouall, M. A. Robb, U. Niazi, F. Bernardi, and H. B. Schlegel, *J. Am. Chem. Soc.*, **109**, 4642 (1987).
- 14) M. Joucla and J. Hamelin, *J. Chem. Res. M.*, **1978**, 352.
- 15) J. J. Tufariello, "Nitrones," in "1,3-Dipolar Cycloaddition Chemistry," ed by A. Padwa, Wiley Interscience, New York (1984), Chap. 9.
- 16) B. Gaede and T. M. Balthazor, *J. Org. Chem.*, **48**, 276 (1983).
- 17) Y. Hanzawa, M. Suzuki, Y. Kobayashi, and T. Taguchi, *J. Org. Chem.*, **56**, 1718 (1991).
- 18) S. Murahashi, H. Mitsui, T. Shiota, T. Tsuda, and S. Watanabe, *J. Org. Chem.*, **55**, 1736 (1990).
- 19) "SAPI91", Fan Hai-Fu (1991), Structure analysis programs with intelligent control, Rigaku Corporation, Tokyo, Japan.
- 20) "DIRDIF92", P. T. Beurskens, G. Admiraal, G. Beurskens, W. P. Bosman, S. Garcia-Granda, R. O. Gould, J. M. M. Smits, and C. Smykalla (1992). The DIRDIF program system, Technical Report of the Crystallography Laboratory, University of Nijmegen, Netherlands.
- 21) "teXsan", Crystal Structure Analysis Package, Molecular Structure Corporation (1985 and 1992).
- 22) "International Tables for X-Ray Crystallography", Kynoch Press, Birmingham, England (1974), Vol. IV.